TRIBHUVAN UNIVERSITY
INSTITUTE OF ENGINEERING
PULCHOWK CAMPUS

THESIS NO:S011/075

Non Linear Damage Accumulation Based Fatigue Life Estimation of Reinforced Concrete Bridges Considering Overloading Effects

by

Prabin Wagle

A THESIS
SUBMITTED TO THE DEPARTMENT OF CIVIL ENGINEERING
IN PARTIAL FULFILLMENT OF THE REQUIREMENTS FOR THE
DEGREE OF MASTER IN
STRUCTURAL ENGINEERING

DEPARTMENT OF CIVIL ENGINEERING
LALITPUR, NEPAL

SEPTEMBER, 2021

TRIBHUVAN UNIVERSITY

INSTITUTE OF ENGINEERING

PULCHOWK CAMPUS

DEPARTMENT OF CIVIL ENGINEERING

The undersigned certify that they have read, and recommended to the Institute of Engineering for acceptance, a thesis entitled " **Non Linear Damage Accumulation Based Fatigue Life Estimation of Reinforced Concrete Bridges Considering Overloading Effects** " submitted by **Prabin Wagle (075MSStE011)** in partial fulfillment of the requirements for the degree of Master of Science in Structural Engineering.

..…………………………………

Supervisor, Dr. Kamal Bahadur Thapa

Department of Civil Engineering

Pulchowk Campus, Institute of Engineering

..…………………………………

External Examiner, Er. Rajendra Raj Sharma

Retd.Superintendent Engineer

Department of Road

..…………………………………

Committee Chairperson, Dr. Kamal Bahadur Thapa

M.Sc Co-ordinator

Department of Civil Engineering

Pulchowk Campus, Institute of Engineering

Date: September,2021

COPYRIGHT

..……………………………………

Head of Department

Department of Civil Engineering

Pulchowk Campus, Institute of Engineering

Lalitpur, Nepal

ABSTRACT

This thesis presents an attempt to determine fatigue life of reinforced concrete bridges by adopting a non-linear damage accumulation method subjected to different amplitude loading due to passing of vehicles in Nepal. The bridge was modeled in finite element software and static analysis was carried out to determine the stresses acting on a bridge deck. The corresponding stresses in reinforcement bars is determined using limit state method and the stresses are incorporated in sequential law to carry out the fatigue life. Since S-N curves available in different codes represents stresses corresponding to more than hundred thousand cycles of failure, a full range S-N curve is developed to carry out sequential law. The material properties of the modeled bridges are taken from design data. The thesis concludes that the fatigue damage due to sequential law is low in previous years; however, there is exponential increase in damage in later years. Although the updated linear method seems to yield almost comparable result as sequential law, the fatigue progress is best represented by sequential law. In addition, the fatigue life for various overloading conditions is determined, and change in damage for respective overloading is analyzed.

ACKNOWLEDGEMENTS

I wish to express my sincere gratitude to my supervisor and our program coordinator Prof. Dr. Kamal Bahadur Thapa, for his continuous guidance, inspiration and encouragement during the thesis work and study period. His lectures and advices proved to be valuable in process of this thesis work.

I would also like to acknowledge all the faculty members of Department of Civil Engineering for the knowledge and concepts they gave me during my study at IOE, Pulchowk Campus.

I am thankful to Roads Board Nepal for providing financial supports to conduct this work. Also, I am thankful to Center for Infrastructure and Development Studies (CIDS) for providing support and knowledge for completion of this study.

I would like to express my sincere gratitude to Asso.Prof Dr Jagat Kumar Shrestha and Ass.Prof Dr Rojee Pradhananga for their invaluable support for completion of this study

I would like to express my very great appreciation to Er. Pradeep Tamang, Er. Nishan Thapa, Er. Pramod Tiwari, Er. Bijay Ban, Er. Nishan Pokhrel and my classmates for their direct and indirect help over the period of master's study as well as this thesis.

I would like to recognize the assistance obtained through the reference books and research papers and would like to thank their authors.

To my family, thank you for encouraging me in all of my dreams and inspiring me during the thesis work.

Prabin Wagle

075/MSStE/011

Sep, 2021

TABLE OF CONTENTS

LIST OF TABLES

LIST OF FIGURES

LIST OF SYMBOLS

D_i	=	Damage state at level i
$\sigma_{(i)eq}$	=	Equivalent stress at level i
σ_i	=	Applied stress at level i
σ_u	=	Ultimate stress
σ_{i+1}	=	Applied stress at level i+1
N_{iR}	=	Failure number of cycles at level i
σ_∞	=	Endurance Limit
σ^f_c	=	Compressive stress in extreme compression fibre of concrete
b	=	Width of bridge deck considered
x_o	=	Distance from extreme compression fibre to neutral axis
h_o	=	Effective depth of bridge deck
m	=	Ratio of steel elastic modulus to concrete elastic modulus (modular ratio)
M^f_{max}	=	Upper limit of fatigue moments
M^f_{min}	=	Lower limit of fatigue moments
A_o	=	Cross sectional area of reinforcement bars
$\Delta\sigma$	=	Stress range
A	=	Fatigue detail coefficient of steel bar
N	=	No of fatigue stress cycles
K	=	Constant value of the slope of the S-N line
f_{ck}	=	Average compressive strength of concrete

LIST OF ABBREVIATIONS

AASHTO	=	American Association of State Highway and Transportation Officials
S-N	=	Stress vs Failure number of cycles
RC	=	Reinforced concrete
ANSYS	=	Analysis of Systems (Software).
SSEA	=	Swiss Society of Engineers and Architects
CSI	=	Computers and Structures, Inc
LL	=	Live Load
IRC	=	Indian Road Congress
BS	=	Bus
2AT	=	Two axle truck
MAT	=	Multi Axle Truck
FAW	=	Front Axle Weight
RAW	=	Rear Axle Weight
Mpa	=	Mega Pascal
DoTM	=	Department of Transport Management

CHAPTER ONE: INTRODUCTION

1.1 Introduction

Transportation infrastructure such as bridges is subjected to repeated cyclic loads throughout their lives that cause fatigue in its structural components. Fatigue, as defined, is the progressive and localized structural damage that occurs due to repeated cyclic loading. Due to continuous repetition of loads fatigue distress occurs and materials like steel undergo brittle failure much before their yield strength is reached. Thus, the nature of loading in bridges can be taken as the major indicator of its performance in fatigue.

In reinforced concrete bridges, deck slabs, which are found to be the most fatigue critical elements for fatigue failure, undergo millions of large load cycles during its service life (Schläfli & Brühwiler, 1998). Deng, Yan, & Nie, (2018) documented a significant reduction in fatigue life of bridge deck considering the coupled corrosion overloading effects. Despite these facts, the prevailing design codes do not consider the effect of fatigue in the design of RC bridge deck slabs. Therefore, research needs to be carried out to determine the service life of RC bridge decks considering overloading condition and fatigue environment.

Different vehicle with different axle weights has different stress impacts on the bridge. The load acting on a bridge is variable in nature. Different vehicle with different axle weights has different stress impacts on the bridge. There have been many studies related to the interaction of lower and higher stress levels in fatigue life estimation. Linear damage accumulation rule recommended by most of the design codes may over-estimate or under estimate fatigue damage in the bridge because it does not consider the loading sequence effect. The fatigue performance of the bridges is different than what Miner's rule estimates. In order to incorporate the load sequence effect, a new damage indicator based sequential law as proposed by Mesmacque, Garcia, Amrouche, & Gonzalez,(2004) is useful to estimate the fatigue life of the RCC bridge.

The repeated cyclic loading being the major factor for fatigue, other external factors also accelerate fatigue phenomena. The rapid increment in traffic density and the existence of overload phenomenon amplifies the stress range in the RCC Bridge deck which obviously cause bridge deck to run a higher risk of fatigue damage. The actual truck loading is far more than it is designed for. The bridges are designed for serviceability with a certain factor of safety for loading however for fatigue evaluation, the overloading of vehicles is not considered. Hence, it is important to consider overloading effects on fatigue life evaluation of the bridge.

Different researches have been carried out for years to have the proper assessment of the estimation of fatigue life of bridges under various circumstances. Stress controlled method, strain-controlled method, and crack propagation method is generally used to assess the fatigue life of various components of bridges. Strain controlled method is considered to be more accurate for low cycle fatigue however bridges are subjected to high cycle fatigue. So, the stress-controlled method is adopted to have fatigue assessment for bridges. Crack propagation method using fracture mechanics seems to provide accurate results but for this, the crack should be monitored from the time when it initiates and it is quite difficult to carry out this process in those bridges that had been built a long time ago. So, in this research, stress monitored fatigue life assessment is adopted.

1.2 Problem Statement/Motivation

The reinforced concrete T-girders comprises almost 50% of bridges built in Nepal. Since the load cycles over the service life is increasing drastically each year, there is a potential cause of structural short service life problem. Hence, the concern in fatigue of concrete bridges is increasing. However, there is still no practice of evaluating fatigue during design of bridges due to complexity in understanding fatigue influence in RCC bridge.

In recent years, various tests on fatigue-induced failure modes have been studied. The influence of fatigue on reinforced concrete is complex phenomenon. (Barnes & Mays, 1999), Yang, Yi, & Li (2017) and Heffernan & Erki (2001) in their different experimental researches concluded the fatigue fracture of tensile reinforcement was dominant factor in governing the failure mode. This result had huge contribution to carry out fatigue life of bridge since the experimental determination of S-N curve was easier for reinforcement bars.

In bridges, damage caused by vehicles of different axle weight is idealized as linear damage of components due to its simplicity in the calculation. So linear damage accumulation theory is used in codes for fatigue life estimation. However, this rule does not incorporate the effect of load sequence. Many types of research have acknowledged the impact of load sequence that arises due to variable amplitude loading. Thus, the result obtained by this method has questionable inaccuracies. In addition to this, external factors like overloading cause a significant change in stress distribution which are generally neglected during fatigue life estimation.

1.3 Purpose and Objectives of the Study

1. To incorporate load sequence effect using new damage indicator based sequential law
2. To determine the impact of overloading on fatigue performance
3. To estimate the fatigue fracture life of the reinforcement bars in RCC bridge.

1.4 Limitations of study

1. For simplifying the number of cycles per vehicle was assumed equal to one cycle per truck.
2. Concrete cracking was ignored in this study.
3. The effect of overloading was considered only in reinforcement bar.
4. The effect of multiple trucks in bridge was ignored.
5. Local stress effect was ignored in this study.
6. Vehicles are assumed to have permissible designed weight.
7. The effect of dead load on mean stress is ignored.

CHAPTER TWO: LITERATURE REVIEW

2.1 General

Many research articles related to fatigue failure modes, approaches of fatigue life estimation, linear as well as non-linear damage effects and overloading models are studied.

2.2 Fatigue Failure Modes

In a reinforced concrete T-girder bridge, there are basically two failure modes: Concrete failure mode and reinforcement bars failure mode. Various experiments were carried out to find out the dominant fatigue failure mode. Barnes & Mays (1999) conducted fatigue tests on five RC girders and showed the dominant one is fatigue fracture in tensile reinforcements. Heffernan & Erki (2001) in their experimental study on twelve girders found out that the specimens failed as a result of brittle fracture of tensile rebars and they succeeded in increasing fatigue life by using carbon fiber plate (CFRP) due to lowering of stresses in rebars. However, their experimental results were based on small scale specimens. Charalambidi, Rousakis, & Karabinis (2016) studied fatigue behavior of large scale reinforced concrete girders and their test results have shown that the girders, even being large size, primarily failed due to tensile fracture of steel rebars. This concludes that the dominant fatigue failure mode of RC girder is tensile fracture of steel rebars and is irrespective of the size of test specimen.

2.3 Approaches to fatigue life estimation

Distinct academics have recognized different techniques to fatigue life assessment. Using a fracture mechanics method, Arteaga, Bressolette, Chateauneuf, & Silva (2008) and Ma, Guo, Wang, & Zhang (2020) proposed a probabilistic model for fatigue life assessment of bridge girders and beams, respectively. This paper included a variety of materials as well as uncertainty about the surroundings. V, R, & A(2015) used a non-linear finite element and the S-N curve to evaluate the fatigue of an RCC bridge. Field strain measurements were used by Alampalli & Lund(2005) and Zhou(2005) to determine fatigue life. Strain gauges were put in various locations to obtain strain and the accompanying stresses. Many alternative ways are defined, but AASHTO defines the core approach. The S-N curve is commonly used to estimate fatigue life, and many researchers have followed suit, determining the failure number of cycles by locating matching stresses operating on the bridge component.

2.4 Damage models

Bridges must bear fluctuating loads throughout the course of their lives, but because calculating this type of load is difficult, these loads are transformed to comparable constant loads using the rain flow counting method. Damage accumulation is also done using Miner's rule, which is a linear damage accumulation rule. However, Siriwardane, Ohga, Dissanayake, & Taniwaki (2007) and Dattoma, Giancane, Nobile, & Panella (2005) discovered that utilizing Miner's rule for variable amplitude loading, life estimates were shown to be incorrect since it does not account for load sequence effects. As a result, novel damage accumulation algorithms that account for non-linearity and load sequence impact have been devised. For variable amplitude loading, Dattoma, Giancane, Nobile, & Panella (2005) suggested a novel non-linear continuum damage model. By assuming a new value for the damage function in the damage model, the model calculates the fatigue damage caused by cycles below the fatigue limit. Mesmacque, Garcia, Amrouche, and Gonzalez (2004) suggested a new damage indicator-based fatigue sequential law. By providing a new damage parameter, damage-induced tension is carried from one level to the next until the ultimate stress is reached. Another continuous damage model proposed by Li, Chan, & Ko (2001) used accumulated microplastic strain and current damage state to develop a damage model. Thus, the results obtained using the sequence effect are more realistic than the linear damage accumulation rule, according to the above-mentioned new damage models.

2.5 Overloading models

Various works have been done for fatigue life considering uncertainty due to vehicle overloading. Wang, Deng, & Shao (2016) considered both effects of dynamic vehicle loading and overloading trucks in a steel bridge for calculating fatigue life. In his research three important parameters road surface condition, vehicle speed, and gross weight were incorporated and the vehicle model was adopted from the AASHTO code. Aggarwal & Parameswaran (2015) incorporated various overload factors on trucks with a different number of axle and studied the fatigue life deduction whereas Deng, Yan, & Nie (2018) considered coupled corrosion-overloading effect which provided better results but still the load sequence effect was not considered which would have further increased the accuracy.

Most of the research work assumes constant amplitude loading for its fatigue life estimation because of its simplicity in the calculation and neglect the load sequence effect. This gives rise to considerable inaccuracy in fatigue life. So, summarizing the researches, it can be concluded that they do not provide the most satisfactory results. To incorporate the limitations, my work will access the fatigue life of bridge subjected to variable amplitude loading where load sequence effect, as well as overloading effect that influences fatigue life significantly, are considered.

Some literature reviews with their respective methodologies are tabulated below:

Table 1. Literature review with respective methodology

Literature Review	Methodology
(Zhongxiang, Tong, Hebdon, & Zhang, 2018)	Crack growth method
(Yang, Yi, & Li, 2017)	A new relation of fatigue range taking some variables from S-N curve and both concrete fatigue and steel fatigue were considered
(Dattoma, Giancane, Nobile, & Panella, 2005)	Non-linear continuum damage mechanics model where differential equation is solved to get the fatigue cycles of failure.
(Adasooriya & Siriwardane , 2014)	Modified S-N curve and sequential law
(Kwon, Frangopol, & Soliman, 2012)	Fracture mechanics approach but stress range were obtained from modified bilinear S-N curve
(Ni, Ye, & Ko, 2010)	Probabilistic method with continuous probabilistic formulation of Miner's rule and strain monitoring data from long term SHM system
(Leitao, Silva, & Andrade, 2012)	S-N curve method using mesh refining techniques in ANSYS
(Deng, Yan, & Nie, 2018)	S-N curve considering coupled corrosion and overloading effect.
(Wang, Deng, & Shao, 2016)	S-N curve method considering road surface interaction and overloading effects.

(V, R, & A, 2015)	S-N curve using SAP 2000 and non linear analysis of element using ANSYS
(Alampalli & Lund, 2005)	Field strain measurement and using AASHTO specification 1990.
(Siriwardane, Ohga, Dissanayake, & Taniwaki, 2007)	New sequential law and updated S-N curve

CHAPTER THREE: METHODOLOGY

A fatigue damage method for evaluating load sequence effect has been proposed. As a suggestion from AASHTO, the S-N curve is used to determine the failure number of cycles. Since AASHTO suggested S-N curve describes stress range corresponding to more than ten thousand failure number of cycles also knows as partial S-N curve so a full range S-N curve is developed using Vechet and Kohout curve modeling technique. The methodology includes:

1. An RCC bridge is selected with consultation from supervisor
2. Geometrical and material properties are determined
3. Average vehicular flow and heavy vehicles flow is counted
4. Finite modeling of the bridge is done and vehicular flow simulation is carried out to determine stresses
5. Limit state method is used to determine stress range
6. Equivalent number of failure cycles is determined using updated S-N curve and sequential law
7. For overloading condition, overloading factors is determined from traffic stations and again updated in finite model

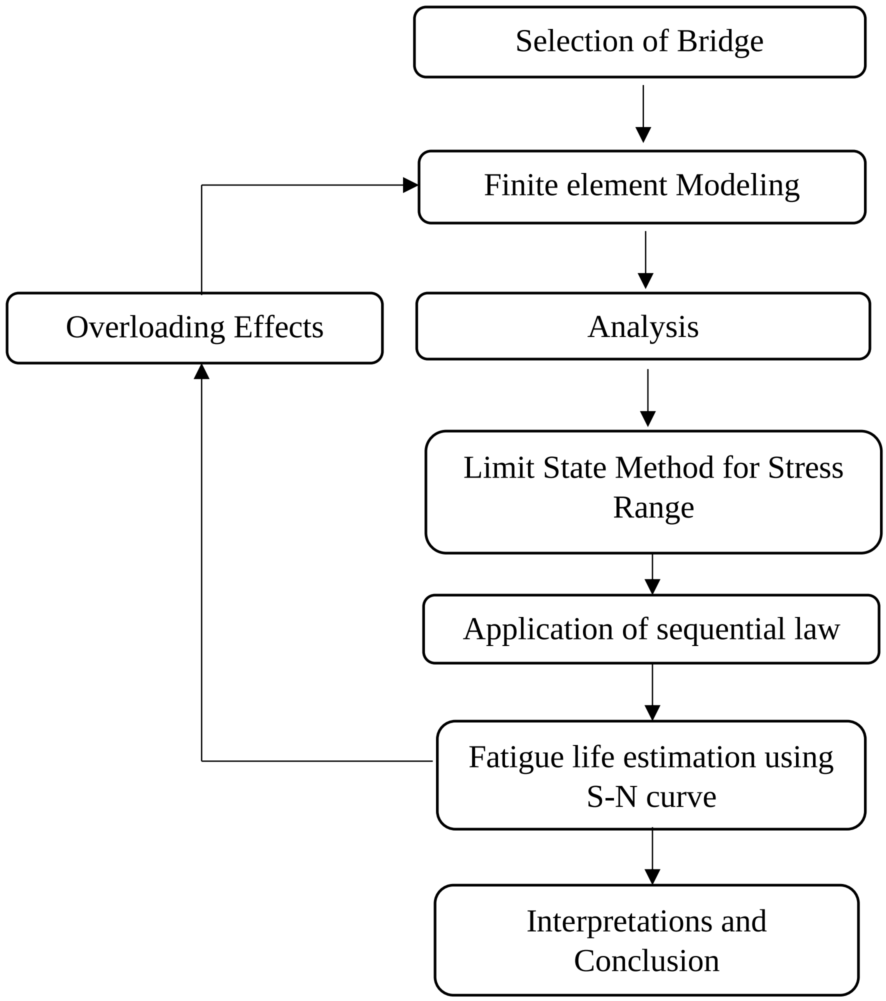

Figure 1. Flow chart of methodology

3.1 Non-Linear Damage Indicator

The most common model to indicate fatigue damage is Miner's rule. However, this model does not take into account the loading history as a result of which, for the same loading condition the experimental results are higher than Miner's expectation for increasing loads and lower for decreasing loads.

The new nonlinear damage indicator is associated with cycles to failure of Wohler curve and experimental results were found to be in accordance with this damage indicator-based results. The damage reported from one stress level is transferred to the next level and this goes on until the component ultimately fails.

A flow chart with an algorithm is shown below:

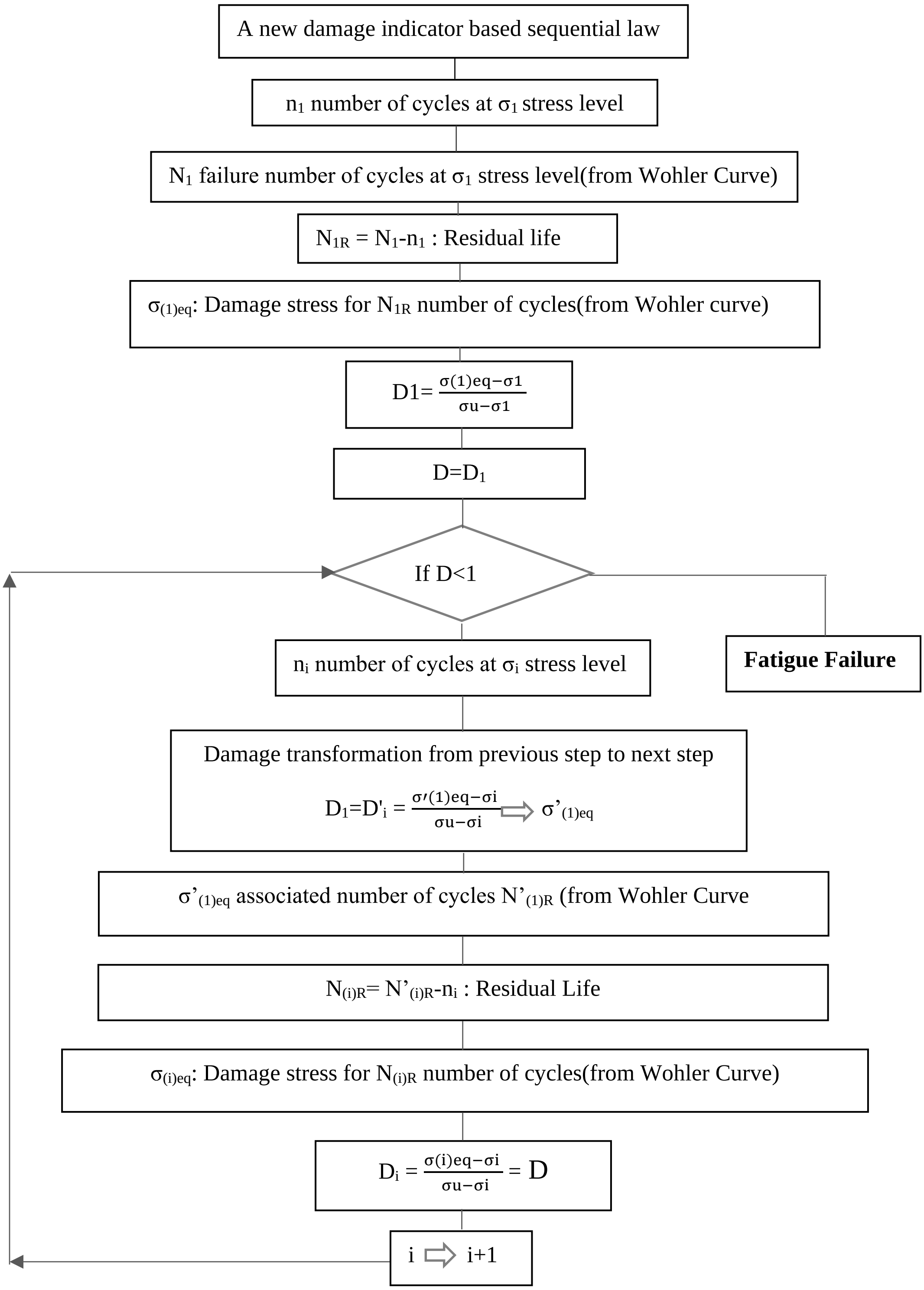

Figure 2. Flow chart for new non-linear damage indicator based sequential law

Suppose a part of component is subjected to certain stress range of σ_i for n_i no of cycles at load level i and N_i is the corresponding failure number of cycles which is obtained from the S-N curve of corresponding component. Hence the residual life at level i can be obtained as (N_i-n_i). A new damage stress $\sigma_{(1)eq}$ is obtained from S-N curve corresponding to failure cycle (N_i-n_i). Here, the damage stress is stress corresponding to remaining life. Now a new damage parameter D_i is introduced, defined as the ratio of increment of damage stress and difference between ultimate and applied stress. The damage indicator is normalized to 1 at failure.

$$\mathrm{Di} = \frac{\sigma(1)\mathrm{eq} - \sigma\mathrm{i}}{\sigma\mathrm{u} - \sigma\mathrm{i}} \qquad 3.1$$

Where,

$\sigma_{(1)eq}$= damage stress

σ_i= applied stress

σ_u= ultimate stress of material

At first cycle, σ_{edi}= σ_i hence D_i=0 and as no of stress cycles increases, the damage approaches to 1. The damage is then transferred to next level i+1 by following relation

$$\mathrm{D1} = \mathrm{D'i} = \frac{\sigma(1)\mathrm{eq} - \sigma\mathrm{i}}{\sigma\mathrm{u} - \sigma\mathrm{i}} = \frac{\sigma'(1)\mathrm{eq} - \sigma(\mathrm{i}+1)}{\sigma\mathrm{u} - \sigma(\mathrm{i}+1)} \qquad 3.2$$

Where

$\sigma'_{(1)eq}$ = damage equivalent stress at level i+1

σ_{i+1} = applied stress at level i+1

We then calculate $\sigma'_{(1)eq}$ and corresponding failure of cycle $N'_{(1)R}$ at level i+1

Now for next step applied stress range of σ_2, and corresponding applied number of cycles n_2, residual cycles of failure is determined as

$$N_{2R} = N'_{(1)R} - n_2 \qquad 3.3$$

With N_{2R} new damage stress $\sigma_{(2)eq}$ is determined and damage is again determined as

$$D_2 = \frac{\sigma(2)eq - \sigma 2}{\sigma u - \sigma 2} \qquad 3.4$$

In the same way the damage is again transferred to next step and same process is carried out until damage is equal to unity.

3.2 Kohout and Vechet Model

In the case of sequential law, it is essential to use full range number of cycles in S-N curve. So the partially known S-N curve is to be developed in full range S-N curve using Kohout and Vechet modelling technique. The procedures are explained below:

Initially, the available partially known curve has to be drawn in the log–log plot. Then draw the three important straight lines:

Line 1: Asymptote $\sigma = \sigma_u$ for the low cycle region (horizontal line across the ultimate strength)

Line 2: Asymptote $\sigma = \sigma_\infty$ for the high cycle region (horizontal line across the fatigue strength)

Line 3: Tangent for the region of finite life described by the equation of partially known curve.

The points of intersection of the tangent (Line 3) with the asymptotes (Line 1 and 2, respectively) occur for N=B and N=C. Hence, the equation of fully known curve can be written as the form of:

$\sigma = \sigma_\infty((N+B)/(N+C))^b$

where b is the slope of tangent in the region of finite life.

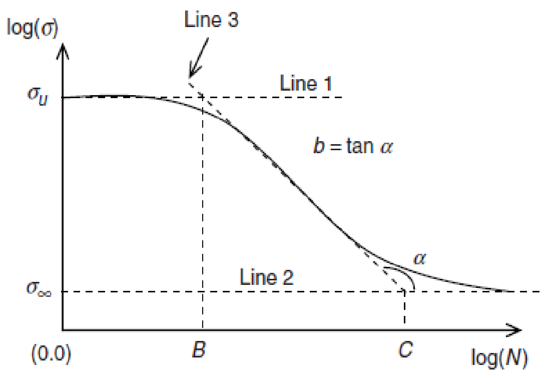

Figure 3: Graphical representation of full range S-N curve using Kohout and Vechet curve modelling technique.

3.3 Stress Range

From finite element method, stress in top compression fiber of concrete is determined which is then used to determine the stress in bars. Considering the equilibrium of internal forces on the failure plane, the maximum moments caused by cyclic loading in the normal section of concrete bridge deck can be determined by:

$$M^f_{max}= 1/2(\sigma^f_c * b * x_0 * (h_o - x_o/3) \quad 3.5$$

$$b * x_o^2/2 - m * A_o(h_o - x_o) = 0 \quad 3.6$$

where

σ^f_c= compressive stress in extreme compression fibre of concrete

b= width of bridge deck considered

x_o= distance from extreme compression fibre to neutral axis

h_o= Effective depth of bridge deck

m= ratio of steel elastic modulus to concrete elastic modulus (modular ratio)

The stress range is then calculated using following equations

$$\Delta\sigma(t)= m*(M^f_{max}- M^f_{min})(h_o-x_o)/I^f(t) \quad 3.7$$

$$I^f(t) = b*x_o^3/3+ m*A_o*(h_o-x_o)^2 \quad 3.8$$

$$b*x_o^2/2- m*A_o*(h_o-x_o) = 0 \quad 3.9$$

where

M^f_{max}= upper limit of fatigue moments

M^f_{min} = lower limit of fatigue moments

A_o= Cross sectional area of reinforcement bars

3.4 S-N curve

The S-N curve of reinforcement bars has been derived from experimental study by Swiss Society of Engineers and Architects (SSEA) in which they proposed an empirical relationship between fatigue stress and number of stress cycles (SSEA, 1997). The relationship is given as

$$\Delta\sigma = \left(\frac{A}{N}\right)^{1/k} \quad 3.10$$

Where,

$\Delta\sigma$= stress range

A = fatigue detail coefficient of steel bar

N= no of fatigue stress cycles

K = constant value of the slope of the S-N line

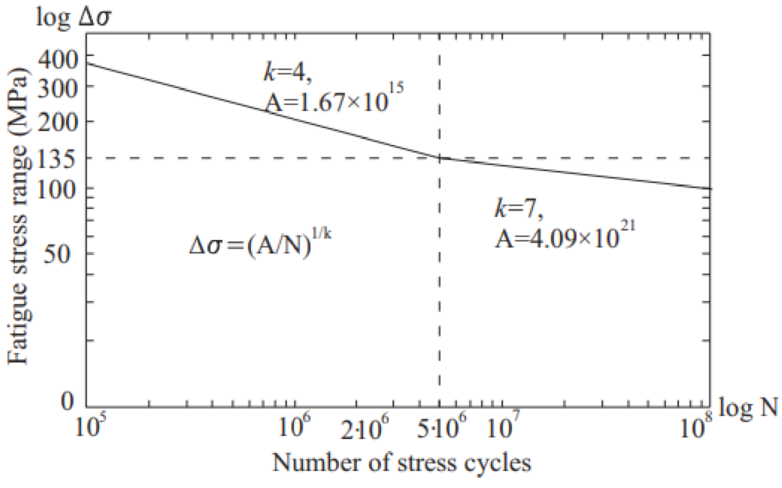

Figure 4 S-N curve of reinforcement bar

CHAPTER FOUR: CASE STUDY

4.1 Structural description

4.1.1 Bridge Model

Bridge Type: Reinforced Concrete Tee Girder Bridge

No of lanes: 2

Total width = 7.5m

Carriage way = 6m (3m each)

Depth of deck = 200 mm

Type of support = Simply supported continuous bridge

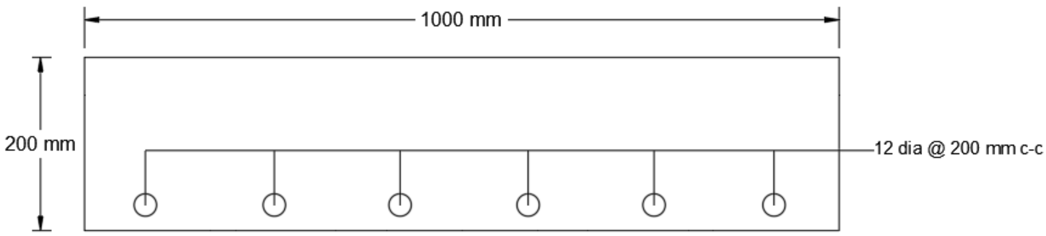

Figure 5: Bridge deck section

4.1.2 Superstructure properties

The super structure consists of three longitudinal girders of rectangular cross section of dimension 2000*350 mm. On each span there are seven cross girders of dimension 1500*250 mm joining longitudinal girders at equal interval of 5m. Thickness of deck slab is 200 mm. The grade of concrete used is M25.

4.1.3 Pier and Cap beam

The bridge consists of two single piers of circular cross section and height of 7.87m including cap beam. The cap beam is rectangular cross section of 2400mm * 1400mm and length of 5900mm. The grade of concrete used is M25.

4.1.4 Abutment

The abutment is of rectangular cross section of dimension 7200 mm*1400mm. The grade of concrete used is M25.

4.2 Finite Element Modelling

The basic objective of finite element modeling is to provide the simplest mathematical formulation of the true bridge behavior. Creating a computer model with finite number of members and finite number of nodal displacements that will represent the behavior of real structure is most critical phase. Several commercial finite element programs are available in the market. CSI Bridge 22 is used in this thesis for modeling the bridge and global finite element model of the standard bridge is shown in the figure.

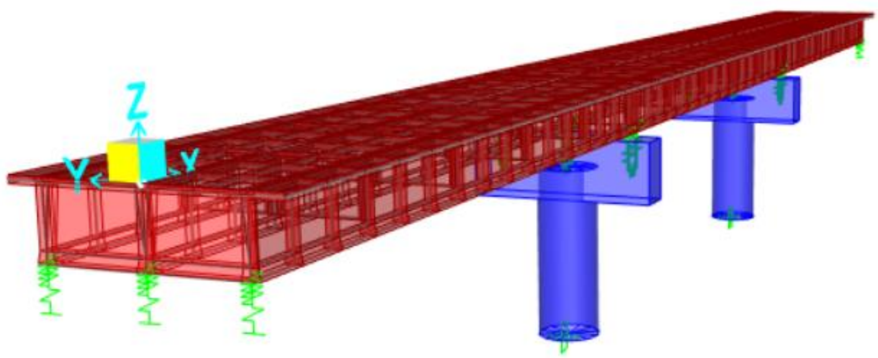

Figure 6 Global Finite Element Model of Bridge

The FE method is highly useful for analyzing problem of complex geometry, materials and boundary conditions. If used properly, we can get reliable result and is cheaper than the experimental testing and analysis. Hence an accurate model is necessary to simulate the actual global structure and accomplish successful analysis.

The Finite Element Method is extensively used in this research to study the stress behavior of RCC T-Girder Bridge. In this study CSI Bridge 22 software is used. Due to its user-friendly interface, the stresses, strains and displacements can be visualized graphically.

In this thesis, multi-step static analysis is carried out. The location of vehicular loading changes and stresses at different loading location is determined to find out the maximum stress at bridge deck.

4.2.1 Material Modeling

Material properties used for the concrete and steel in the Finite Element Analysis are taken from the designed data. The average compressive strength of concrete (f_{ck}) is taken as 25 Mpa. For concrete, a Poisson's ratio of 0.2 was assumed and modulus of elasticity of concrete is calculated as per IS 456-2000 i.e. $5000\sqrt{f_{Ck}}$. The unit weight of concrete is taken as 25 KN/m^3. The yield strength of reinforcement bars is taken as 415Mpa and ultimate strength is taken as 485Mpa. The modulus of elasticity of reinforcement steel is 200,000 Mpa and Poisson's ratio is taken as 0.3. The mass density of steel is 7850kg/m^3.

4.2.2 Boundary Conditions

The bridge is analyzed as simply supported bridge. At abutments, the nodal translations are restrained along vertical axis and the axis which is normal to layout line in the same horizontal plane. At bents, the nodal translations are restrained along vertical axis, along layout line and the axis normal to layout line. Moments are released in all direction in abutments as well as bents.

4.2.3 Geometric Modeling

CSI Bridge 22 is used to carry out the Finite Element Analysis. The bridge deck is modelled by using thin shell elements. The cap bents are modelled by using beam elements whereas the pier and abutment is modelled by using column elements.

4.2.4 Loadings

Different vehicles of respective sizes and axle loads are applied in the finite element software. Point load is assumed for vehicles as local effect due to tyre size is not considered.

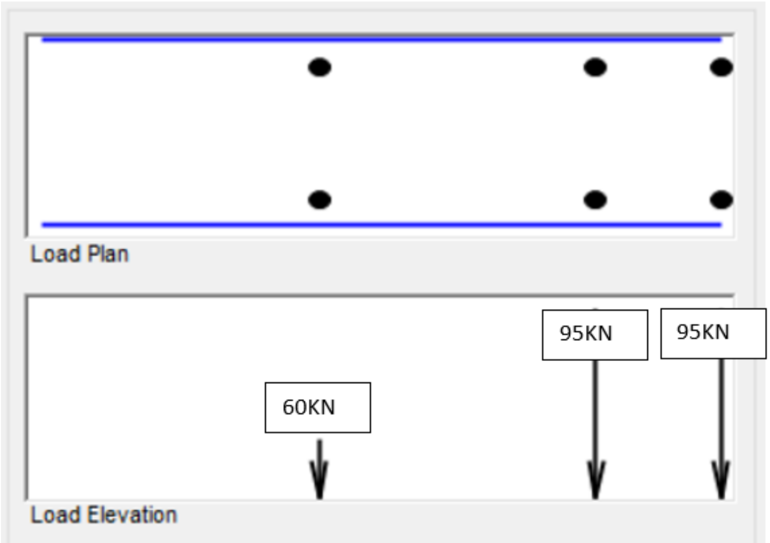

Figure 7: Loading diagram for LPK 2518

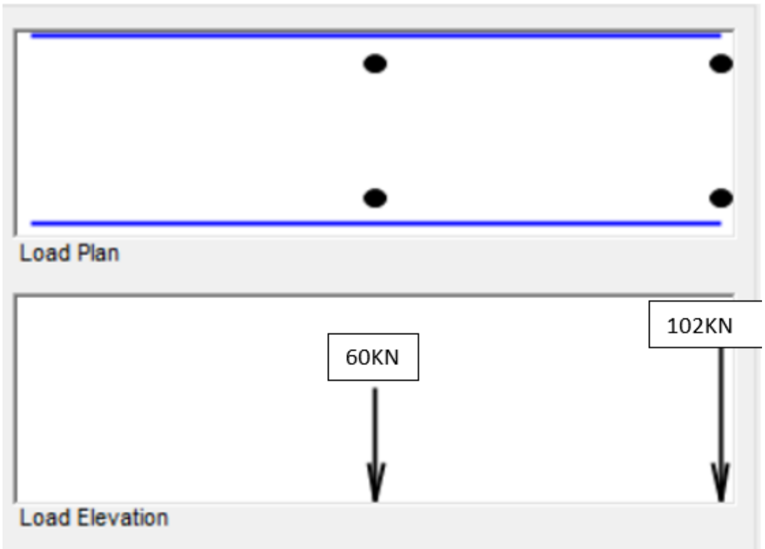

Figure 8: Loading diagram for LPK 1613

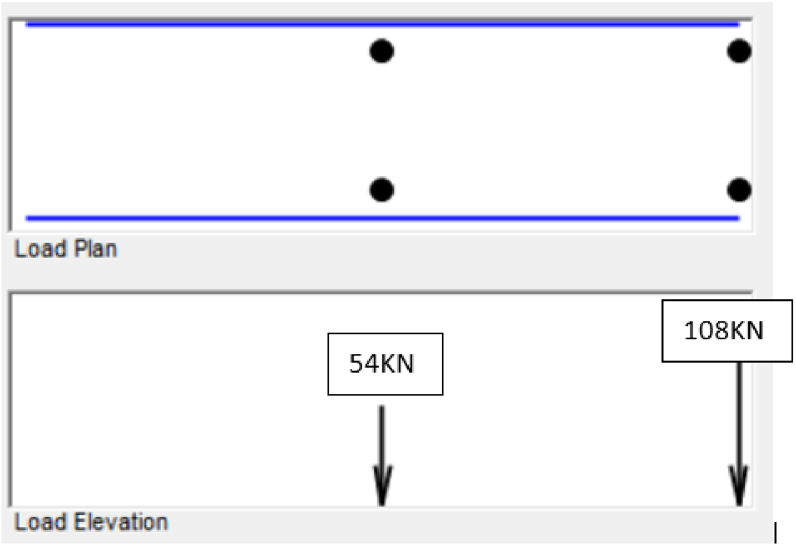

Figure 9: Loading diagram for LPO 1618

4.3 Validation

In this section, the model was verified and is compared with the established result to validate the present model. It was compared with the result of (Pokhrel, 2013). The comparison are as follows:

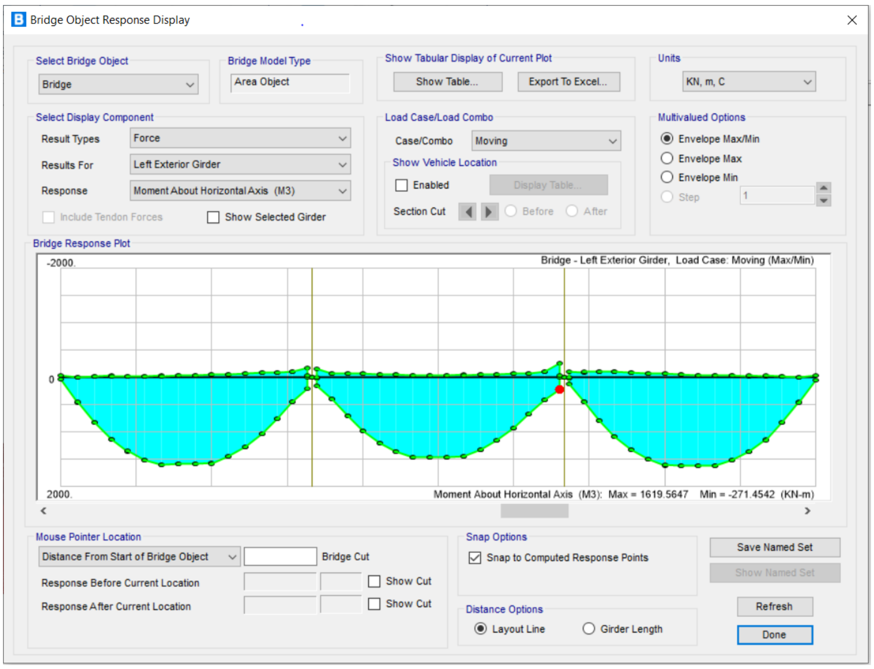

Figure 10: Bending Moment Diagram for LL(Envelope)

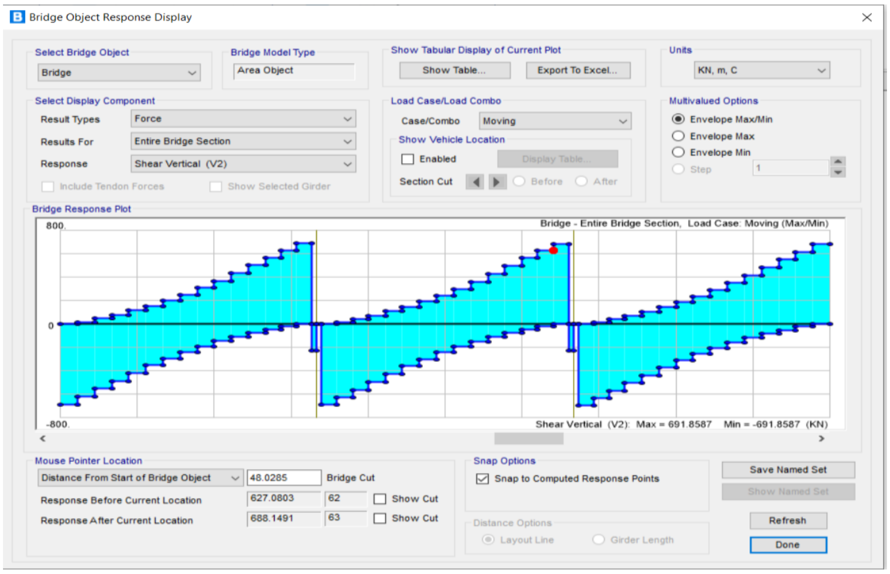

Figure 11: Shear Force Diagram for LL (Envelope)

Table 2: Comparison Table

	Results from Pokhrel	Current Results	Percentage Error
Live Load Bending Moment (IRC Class A)	1592.25 KNm	1619.5647 KNm	1.715%
Live Load Shear Force (IRC Class A)	294KN	282.95 KN	3.75%

4.4 Vehicles

Annual Average daily traffic = 26733 pcu

Average no of multi axle trucks = 1387

Average no of double axle truck = 2595

Average no of buses = 1205

Average yearly increment of vehicles = 3%

The types of vehicles used for study are tabulated below:

Table 3 Vehicle details

Vehicle Type	Bus (BS)	2AT	MAT
Vehicle Name	LPO1618	LPK1613	LPK2518
Wheel base	6.3 m	3.58 m	3.88 & 4.88 m
Total length of vehicle	12 m	6.365 m	7.08 m
Width of vehicle	2.6 m	2.115 m	2.44 m
Max permissible FAW	54 KN	60 KN	60 KN
Max permissible RAW	108 KN	102 KN	190 KN

CHAPTER FIVE: RESULTS AND DISCUSSIONS

5.1 S-N curve

From experimental study by Swiss Society of Engineers and Architects (SSEA) in which they proposed an empirical relationship between fatigue stress and number of stress cycles (SSEA, 1997). The relationship is given as

$$\Delta\sigma = \left(\frac{A}{N}\right)^{1/k}$$

It has been experimentally verified that the slope of the S-N curve changes at 5*10^6 failure number of cycles. The experimental curve is given in figure 4.

Stress and their corresponding failure number of cycles of reinforcing bars are tabulated below:

Table 4 S-N curve data for reinforcing bars

Stress(Mpa)	Failure no of cycles
359.48	1.00E+05
302.29	2.00E+05
254.19	4.00E+05
229.69	6.00E+05
213.75	8.00E+05
202.15	1.00E+06
169.99	2.00E+06
142.94	4.00E+06
135.19	5.00E+06
128.68	7.00E+06
122.29	1.00E+07
104.53	3.00E+07
97.17	5.00E+07
92.61	7.00E+07
88.01	1.00E+08

For the development of full range S-N curve the kohout and vechet modeling yields equation which is expressed below:

The equation of stress and failure no of cycles for full range S-N curve is developed as

$$\sigma = 63.34\left(\frac{N + 14259.12}{N + 10\text{^}9}\right)^{-0.189} \qquad 5.1$$

Where,

σ = stress range

N= failure no of cycles

Table of stress and failure no of cycles after vechet and kohout modelling are presented below:

Table 5 Full range S-N curve data

Stress(Mpa)	Failure no of cycles
580.2899	1.00E+00
580.2592	5.00E+00
580.1055	2.50E+01
579.3412	1.25E+02
575.6117	6.25E+02
558.9661	3.13E+03
504.5639	1.56E+04
407.6403	7.81E+04
308.3131	3.91E+05
228.689	1.95E+06
168.9201	9.77E+06
124.7359	4.88E+07
92.36032	2.44E+08
69.31989	1.22E+09
54.75295	6.10E+09
48.08825	3.05E+10
46.13013	1.53E+11
45.69232	7.63E+11

The full range S-N curve from above data is shown in graph as below:

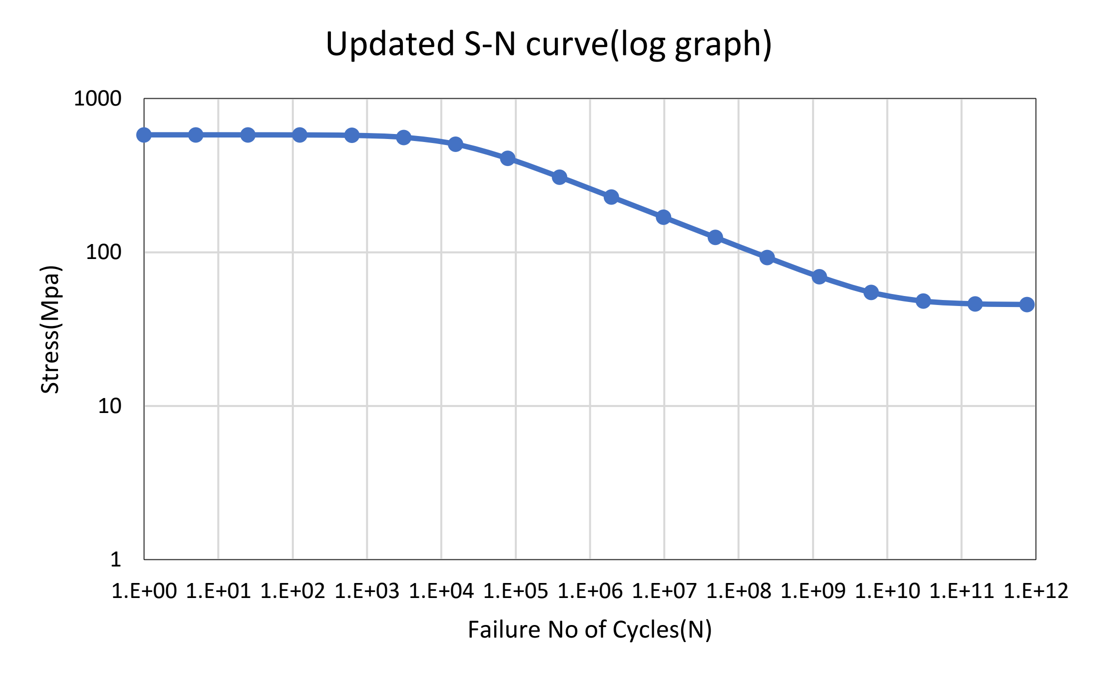

Figure 12: Full Range S-N curve for reinforcing bar

5.2 Stress History

The stresses in top fiber of concrete in bridge deck is calculated and equivalent stress is calculated in reinforcement bar for Multi axle Truck (LPK 2518) and tabulated in *Table 6.*

Table 6: Stress History for LPK 2518

Time Step(s)	Stress (Mpa)	Time Step(s)	Stress (Mpa)
0.1	0.0	1.6	-21.0
0.2	-3.8	1.7	-9.9
0.3	-8.1	1.8	-0.6
0.4	-19.3	1.9	1.6
0.5	-34.9	2	0.7
0.6	-50.6	2.1	0.0
0.7	-66.1	2.2	0.0
0.8	-81.6	2.3	0.0
0.9	-90.1	2.4	0.0
1	-97.8	2.5	0.0
1.1	-91.9	2.6	0.0
1.2	-77.9	2.7	0.0
1.3	-63.8	2.8	0.0
1.4	-49.5	2.9	0.0
1.5	-34.9	3	0.0

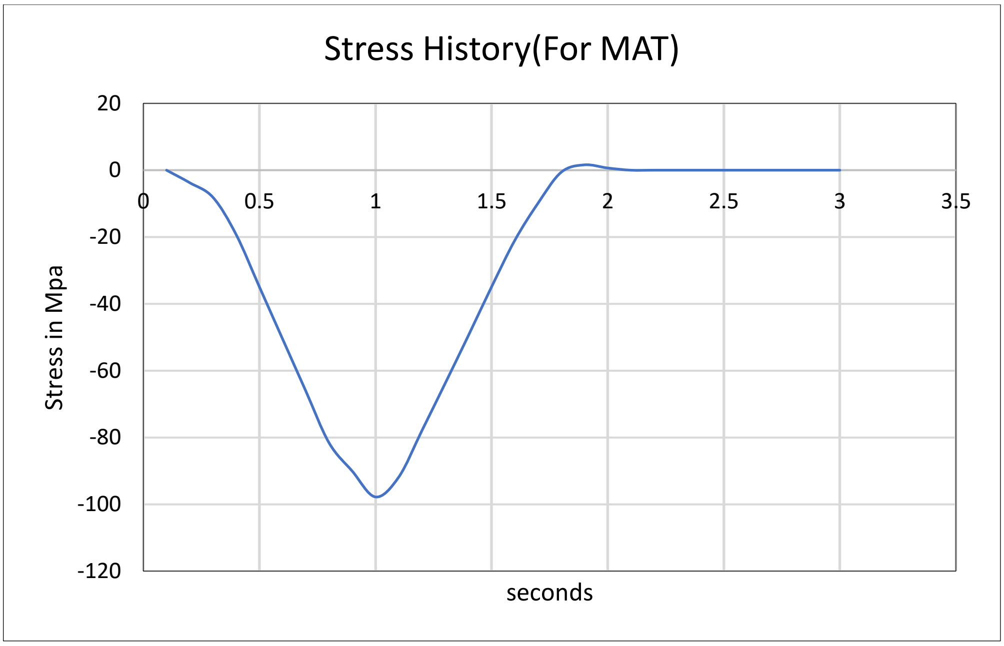

Figure 13: Stress History for Multi Axle Truck

The graph of stress in reinforcement bar and time for multi axle truck is plotted and represented in Figure *13*.

The stresses in top fiber of concrete in bridge deck is calculated and equivalent stress is calculated in reinforcement bar for Two Axle Truck (LPK 1613) and tabulated in Table *7*

Table 7: Stress History for LPK 1613

Time Step(s)	Stress (Mpa)	Time Step(s)	Stress (Mpa)
0.1	0.0	1.6	-11.6
0.2	-4.4	1.7	-4.7
0.3	-8.8	1.8	2.4
0.4	-19.6	1.9	0.9
0.5	-31.5	2	0.2
0.6	-43.3	2.1	0.0
0.7	-55.1	2.2	0.0
0.8	-66.8	2.3	0.0
0.9	-70.3	2.4	0.0
1	-74.3	2.5	0.0
1.1	-65.3	2.6	0.0
1.2	-54.7	2.7	0.0
1.3	-43.9	2.8	0.0
1.4	-33.0	2.9	0.0
1.5	-21.8	3	0.0

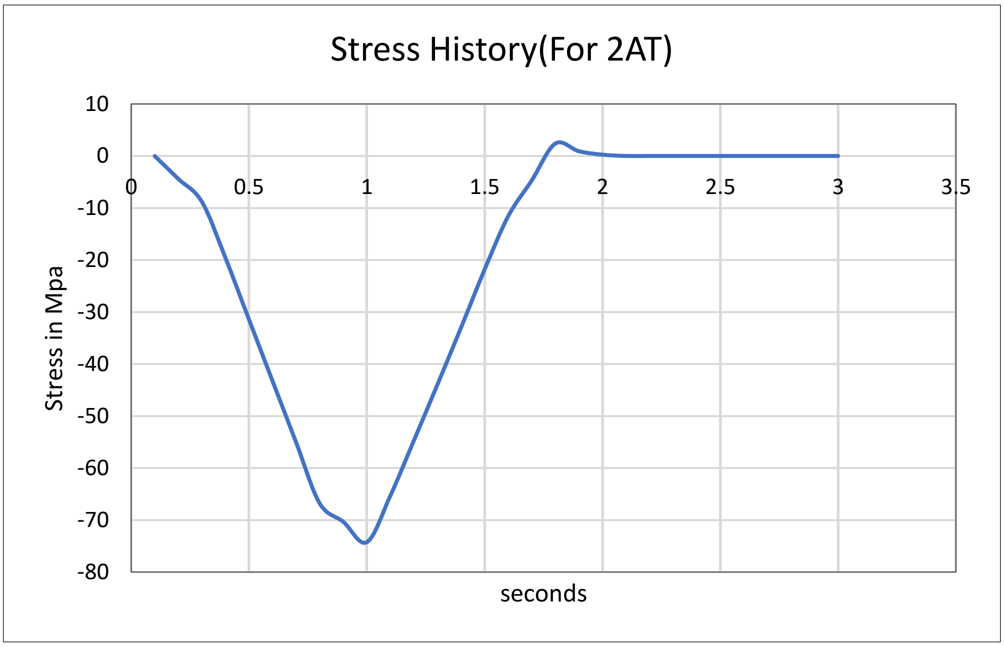

Figure 14: Stress History of Two Axle Truck

The graph of stress in reinforcement bar and time for multi axle truck is plotted and represented in Figure *14*.

The stresses in top fiber of concrete in bridge deck is calculated and equivalent stress is calculated in reinforcement bar for Bus (LPO 1618) and tabulated in Table *8*

Table 8: Stress History for LPO 1618

Time Step(s)	Stress (Mpa)	Time Step(s)	Stress (Mpa)
0.1	0.0	1.6	-24.4
0.2	-4.0	1.7	-17.4
0.3	-7.9	1.8	-10.1
0.4	-11.9	1.9	-2.6
0.5	-17.6	2	1.2
0.6	-29.4	2.1	0.5
0.7	-41.3	2.2	0.0
0.8	-53.0	2.3	0.0
0.9	-57.4	2.4	0.0
1	-61.8	2.5	0.0
1.1	-66.0	2.6	0.0
1.2	-67.4	2.7	0.0
1.3	-56.3	2.8	0.0
1.4	-45.5	2.9	0.0
1.5	-34.6	3	0.0

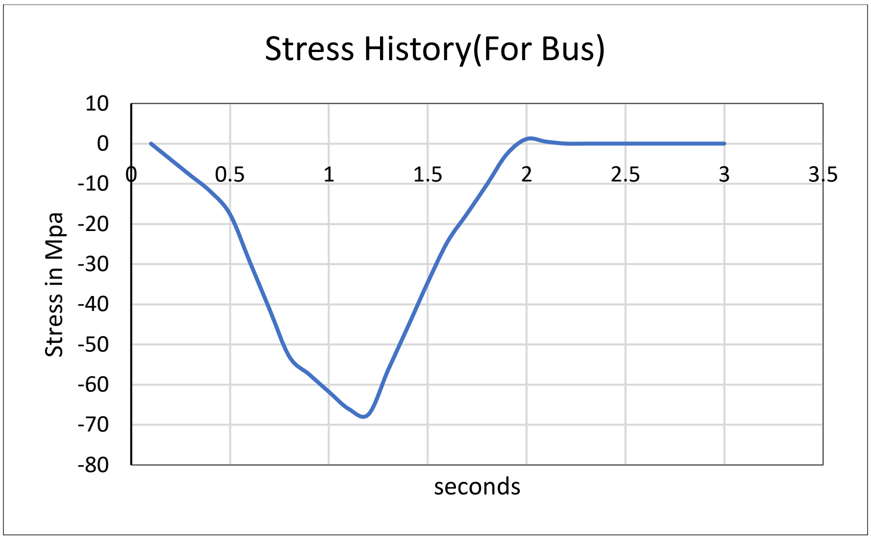

Figure 15: Stress History of Bus

The graph of stress in reinforcement bar and time for multi axle truck is plotted and represented in *Figure 15*

5.3 Stress Range

The stress range for different vehicles passing through the bridge is represented in *Table 9.*

Table 9:Stress Ranges of different vehicles

For LPK 2518 (Multi Axle Truck)	97.79 Mpa
For LPK 1613(2 Axle Truck)	74.26 Mpa
For LPO 1618(Heavy Bus)	67.41 Mpa

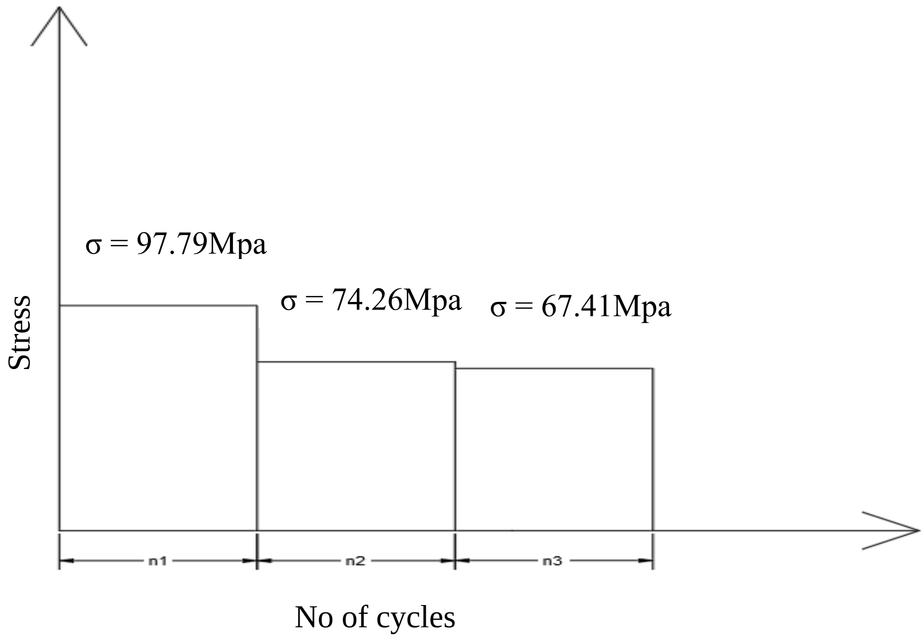

Figure 16: Loading condition

5.4 Fatigue Damage

The damage for sequential method and Miner's method is calculated and damage for interval of 5 years is calculated and tabulated. The fatigue life is estimated when the damage reaches unity.

Table 10: Damage by Sequential law and Miner's rule and updated linear method

Damage					
No of Years	Sequential	No of Years	Miners	No of Years	Updated Linear
5	0.001	5	0.042	5	0.030
10	0.002	10	0.086	10	0.060
15	0.004	15	0.131	15	0.091
20	0.005	20	0.177	20	0.124
25	0.007	25	0.225	25	0.157
30	0.008	30	0.274	30	0.191
35	0.010	35	0.324	35	0.226
40	0.012	40	0.376	40	0.263
45	0.014	45	0.430	45	0.300
50	0.017	50	0.485	50	0.339
55	0.019	55	0.542	55	0.378
60	0.023	60	0.600	60	0.419
65	0.026	65	0.661	65	0.461
70	0.030	70	0.723	70	0.505
75	0.035	75	0.787	75	0.549
80	0.041	80	0.853	80	0.595
85	0.048	85	0.920	85	0.643
90	0.057	90	0.990	90	0.692
95	0.069	95	1.062	95	0.742
100	0.087			100	0.794
105	0.119			105	0.847
106	0.129			106	0.858
107	0.142			107	0.869
108	0.160			108	0.881
109	0.186			109	0.893
110	0.235			110	0.905
111	0.504			111	0.918
112	0.820			112	0.931
113	1.020			113	0.945
				114	0.959
				115	0.973
				116	0.988
				117	1.003

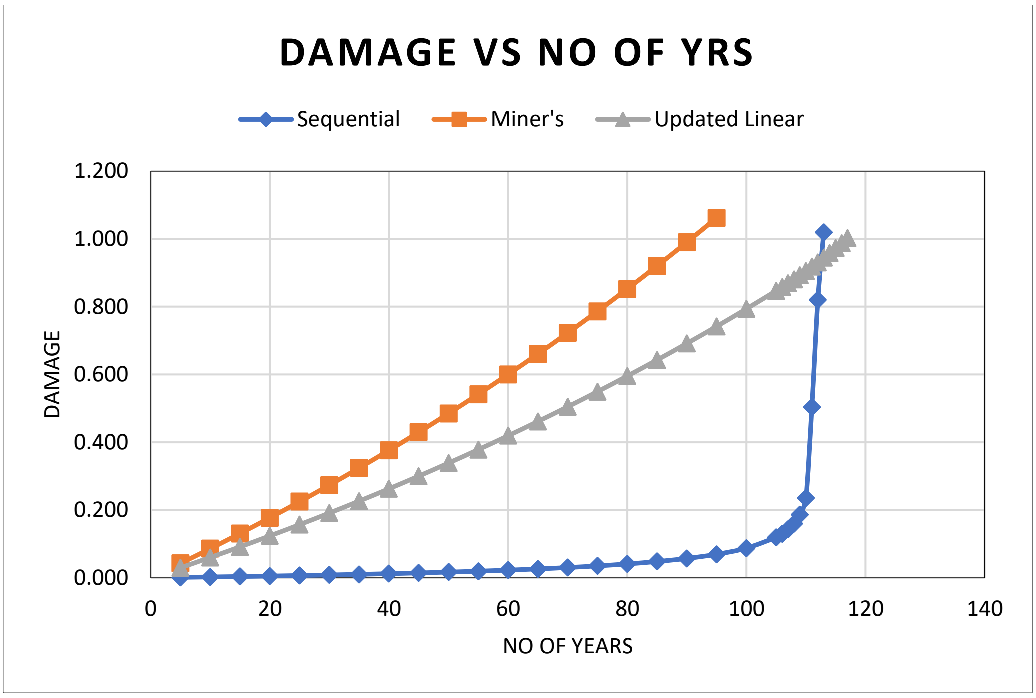

Figure 17: Damage vs Fatigue Life

The fatigue life calculated from various approaches are tabulated and compared in the form of bar diagram.

Table 11: Comparison Table of fatigue life

	Sequential Law	Miner's Law	Updated Linear
Fatigue Life	113 yrs	91 yrs	118 yrs

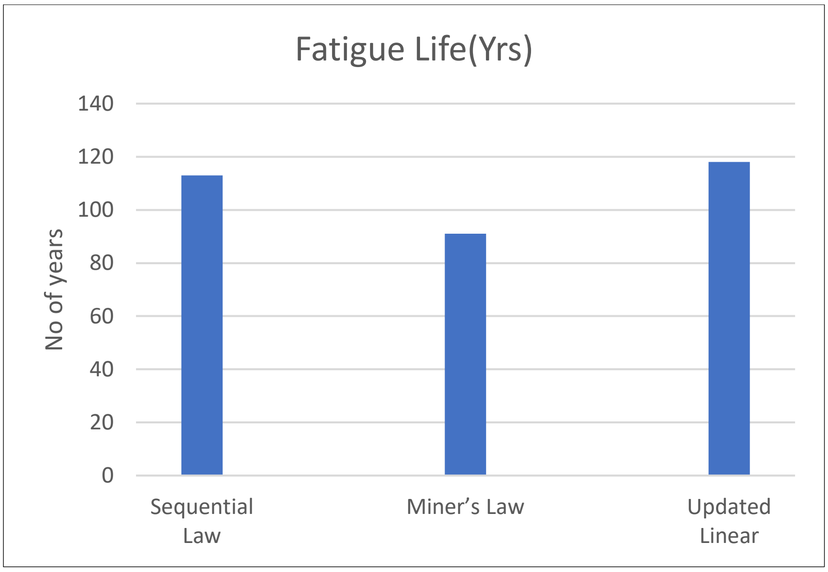

Figure 18: Comparison chart for fatigue life

5.5 Fatigue damage for overloading cases

The different vehicle model taken for the analysis, in real field, are overloaded to a great extent. The impact of overloading for different overloading condition are carried out and compared.

5.5.1 10% overloading case

The axle load of each vehicle used for the analysis are increased by 10% and stresses are determined. The corresponding stresses in reinforcement bars are determined and are embedded in sequential law to carry out non-linear analysis of fatigue life. The corresponding stresses are shown in Figure 19 and fatigue damage is represented in Figure *20*:

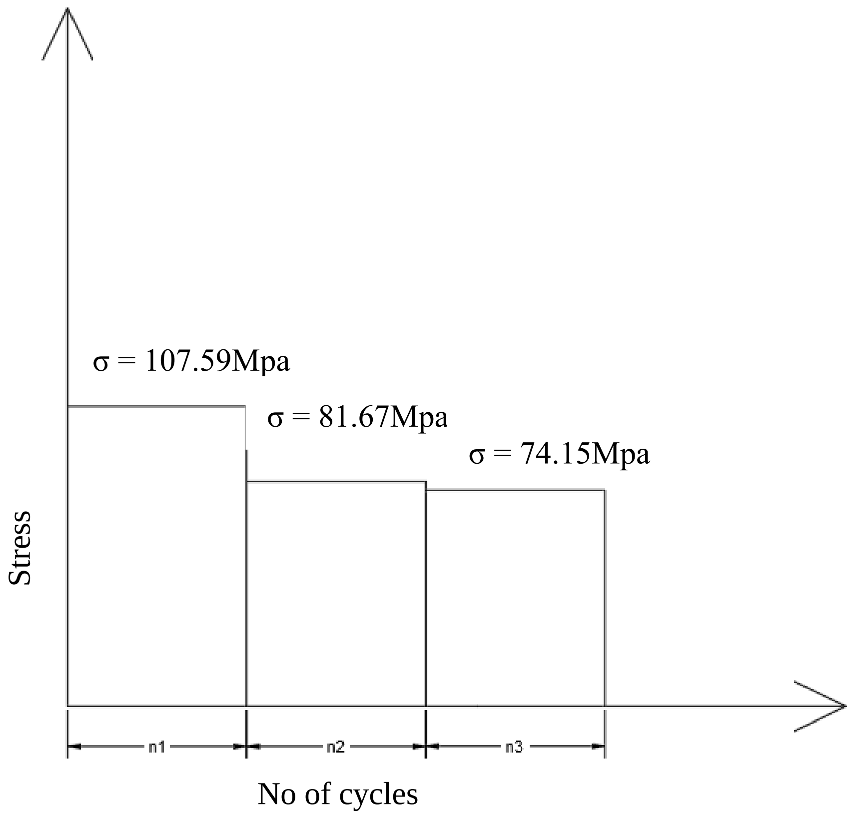

Figure 19: Loading condition

Table 12:Damage by sequential law and Miner's rule for 10% overloading

Damage					
No of Years	Sequential	No of Years	Miners	No of Years	Updated Linear
5	0.003	5	0.082	5	0.055
10	0.005	10	0.167	10	0.112
15	0.008	15	0.255	15	0.170
20	0.012	20	0.345	20	0.230
25	0.016	25	0.438	25	0.292
30	0.021	30	0.534	30	0.356
35	0.026	35	0.632	35	0.422
40	0.033	40	0.733	40	0.489
45	0.041	45	0.838	45	0.559
50	0.052	50	0.946	50	0.631
55	0.067	55	1.056	55	0.705
60	0.089			60	0.781
65	0.133			65	0.859
66	0.148			66	0.875
67	0.169			67	0.892
68	0.203			68	0.909
69	0.273			69	0.927
69.5	0.600			69.5	0.936
70	0.800			70	0.945
70.5	1.013			70.5	0.955
				71	0.965
				71.5	0.975
				72	0.986
				72.5	0.997
				73	1.008

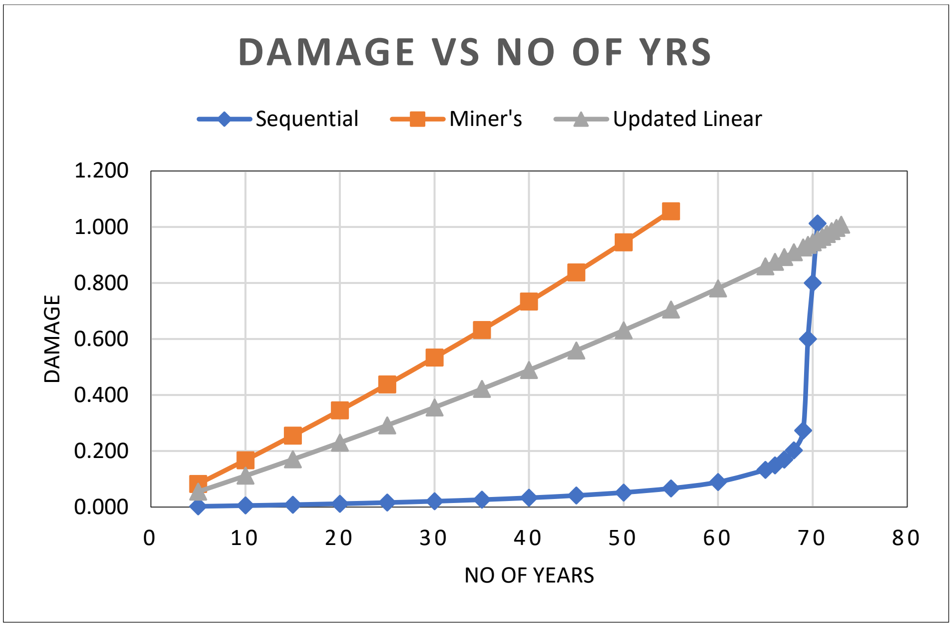

Figure 20: Damage vs fatigue life for 10% overloading

5.5.2 25% overloading case

The axle load of each vehicle used for the analysis are increased by 25% and stresses are determined. The corresponding stresses in reinforcement bars are determined and are embedded in sequential law to carry out non-linear analysis of fatigue life. The corresponding stresses are shown in Figure 21 and fatigue damage is represented in Figure *22*:

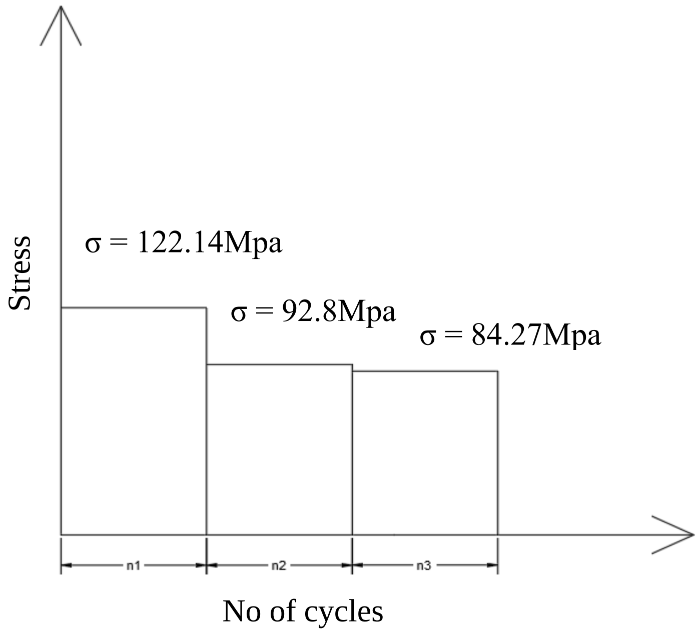

Figure 21: Loading condition

Table 13:Damage by sequential law and Miner's rule for 25% overloading

Damage					
No of Years	Sequential	No of Years	Miners	No of Years	Updated Linear
5	0.007	5	0.201	5	0.117
10	0.015	10	0.408	10	0.237
15	0.026	15	0.621	15	0.361
20	0.040	20	0.840	20	0.489
25	0.061	25	1.066	25	0.620
30	0.096	30	1.299	30	0.755
35	0.204			35	0.895
36	0.289			36	0.923
36.5	0.439			36.5	0.938
37	0.500			37	0.954
37.5	0.680			37.5	0.969
38	0.870			38	0.985
38.5	1.012			38.5	1.002
				39	1.019

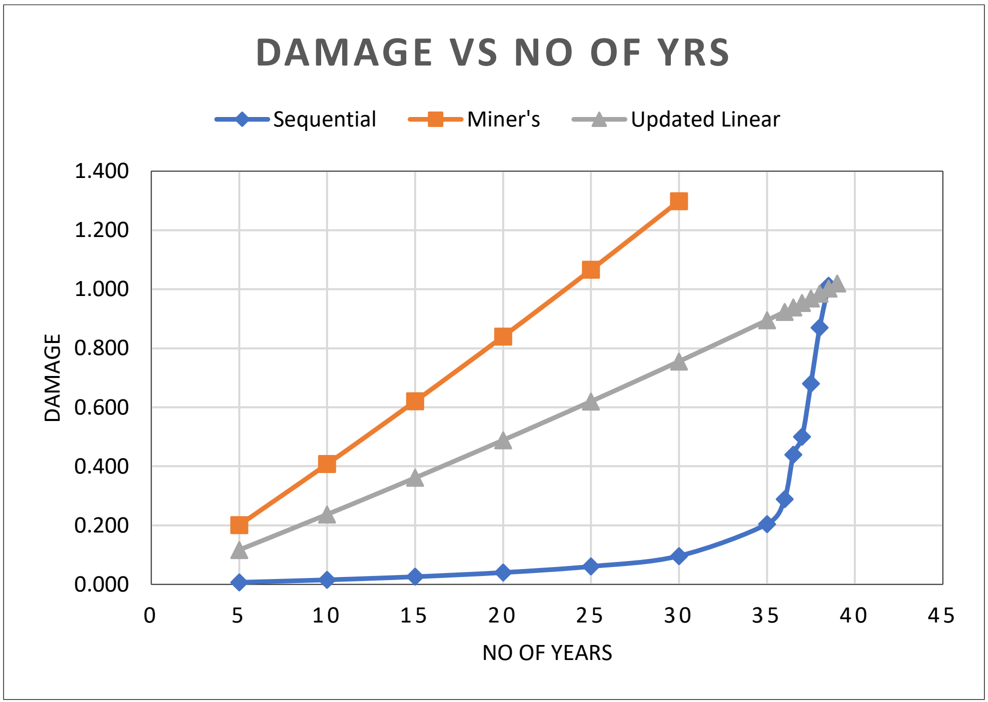

Figure 22:Damage vs fatigue life for 25% overloading

5.5.3 50% overloading case

The axle load of each vehicle used for the analysis are increased by 50% and stresses are determined. The corresponding stresses in reinforcement bars are determined and are embedded in sequential law to carry out non-linear analysis of fatigue life. The corresponding stresses are:

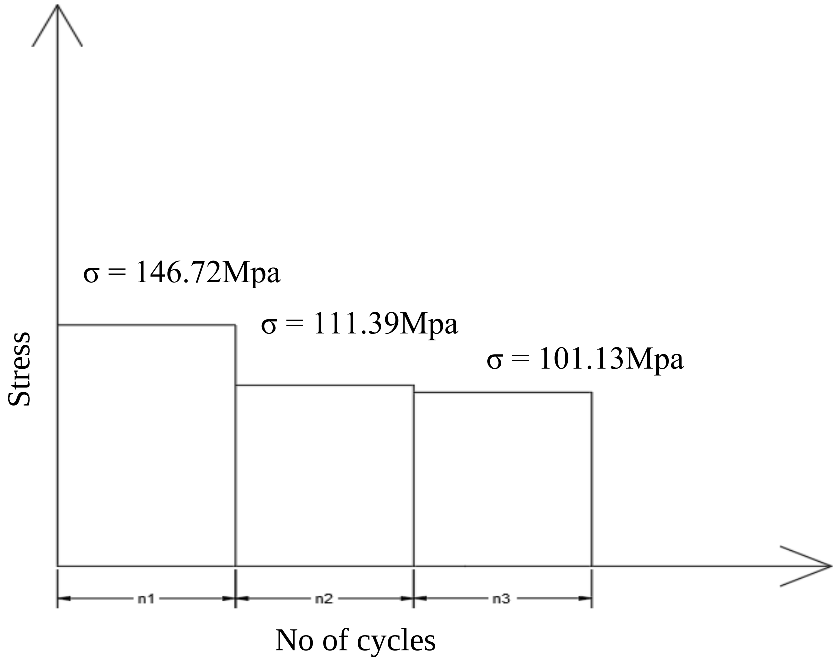

Figure 23: Loading condition

Table 14:Damage by sequential law and Miner's rule for 50% overloading

Damage					
No of Years	Sequential	No of Years	Miners	No of Years	Updated Linear
0	0	0	0	0	0
5	0.030	5	0.724	5	0.323
10	0.092	10	1.469	10	0.656
11	0.115			11	0.724
12	0.151			12	0.795
13	0.221			13	0.867
13.5	0.303			13.5	0.905
14	0.500			14	0.943
14.5	0.800			14.5	0.983
15	1.020			15	1.024

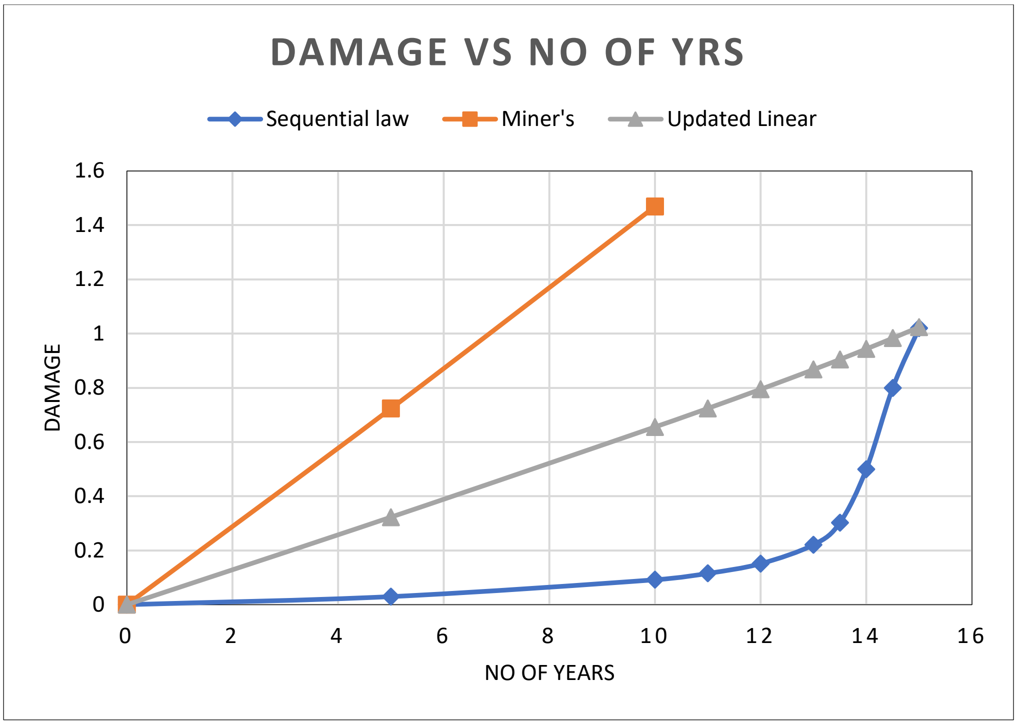

Figure 24:Damage vs fatigue life for 50% overloading

5.5.4: Overloading case for Nepal

Department of Transport Management under Ministry of Physical Infrastructure and Transport has carried out a report on axle load control along national highways (Department of Transport Management, 2021). Results of traffic volume and axle load surveys carried out by the DoTM in 2016 along Prithvi Highway (Naubishe/ Dharke Dhading) is taken as representative traffic volume and level of loading in typical road of Nepal.

The result of the survey shows that for heavy trucks (legal load limit= 16.2 ton), average overloading weight is 1.21 ton which is 7.46%. Similarly, for multi axle truck (legal load limit = 25 ton), average overloading weight is 7.44 ton which is 29.46%. These values are incorporated to get the fatigue life of bridge.

Table 15:Damage by sequential law and Miner's rule for overloading case of Nepal

Damage					
No of Years	Sequential	No of Years	Miners	No of Years	Updated Linear
5	0.007	5	0.205	5	0.106
10	0.015	10	0.416	10	0.215
15	0.025	15	0.633	15	0.327
20	0.039	20	0.857	20	0.443
25	0.057	25	1.087	25	0.562
30	0.086			30	0.685
35	0.147			35	0.811
36	0.171			36	0.837
37	0.210			37	0.864
38	0.295			38	0.892
38.5	0.449			38.5	0.906
39	0.680			39	0.921
39.5	0.840			39.5	0.936
40	0.960			40	0.951
40.2	1.005			40.5	0.967
				41	0.984
				41.5	1.001

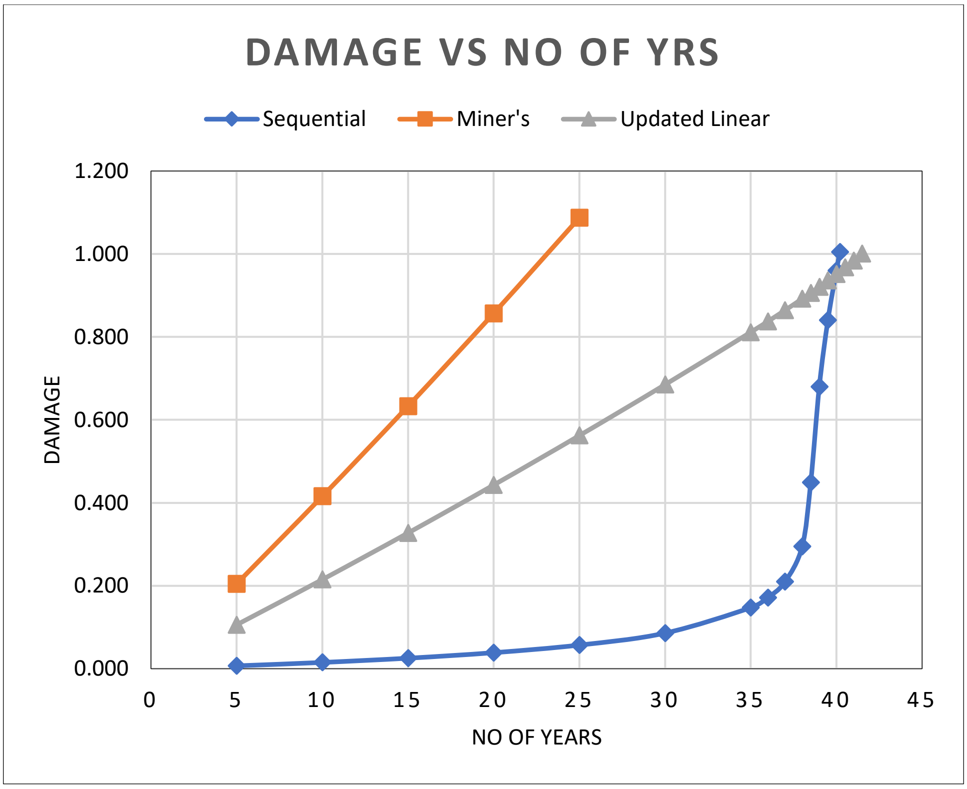

Figure 25:Damage vs fatigue life for overloading condition of Nepal

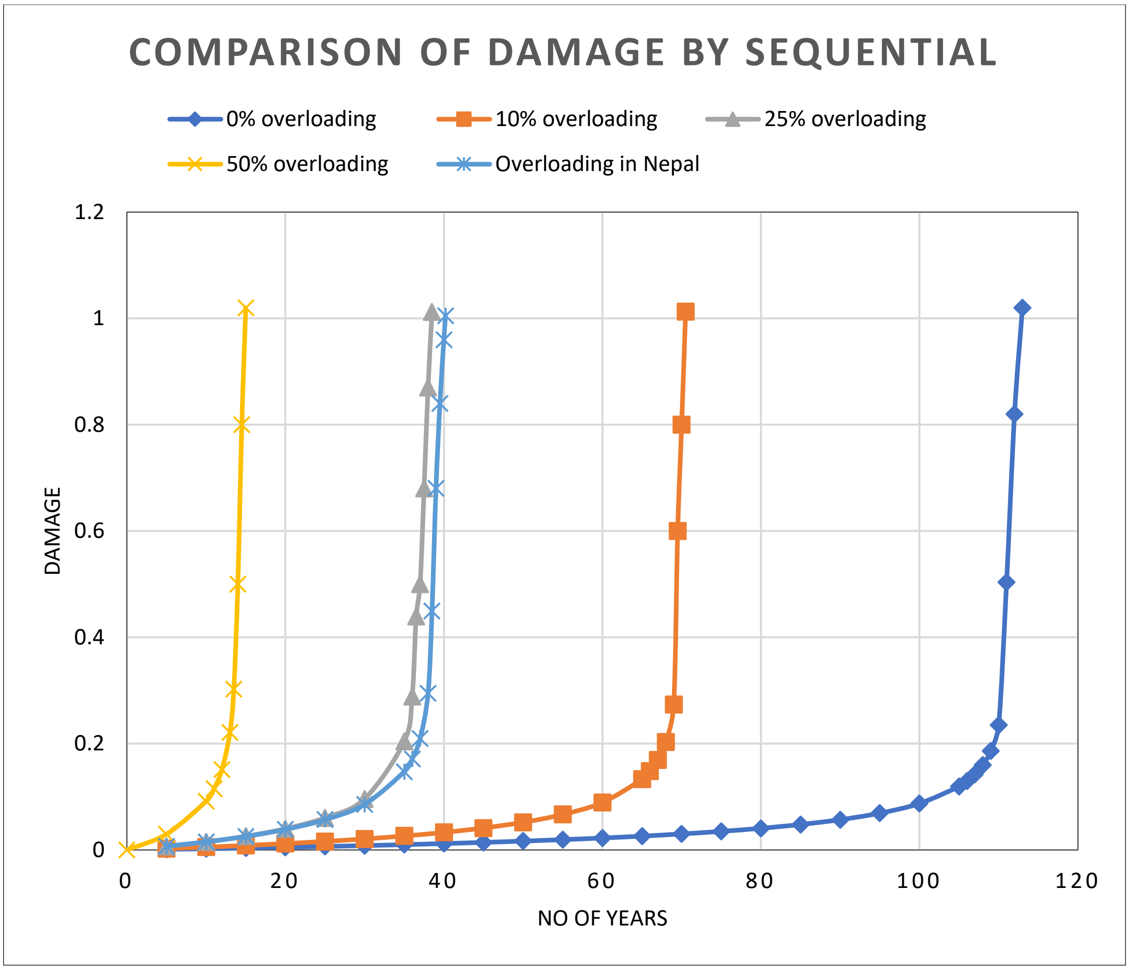

Figure 26: Fatigue life for different overloading condition for sequential law

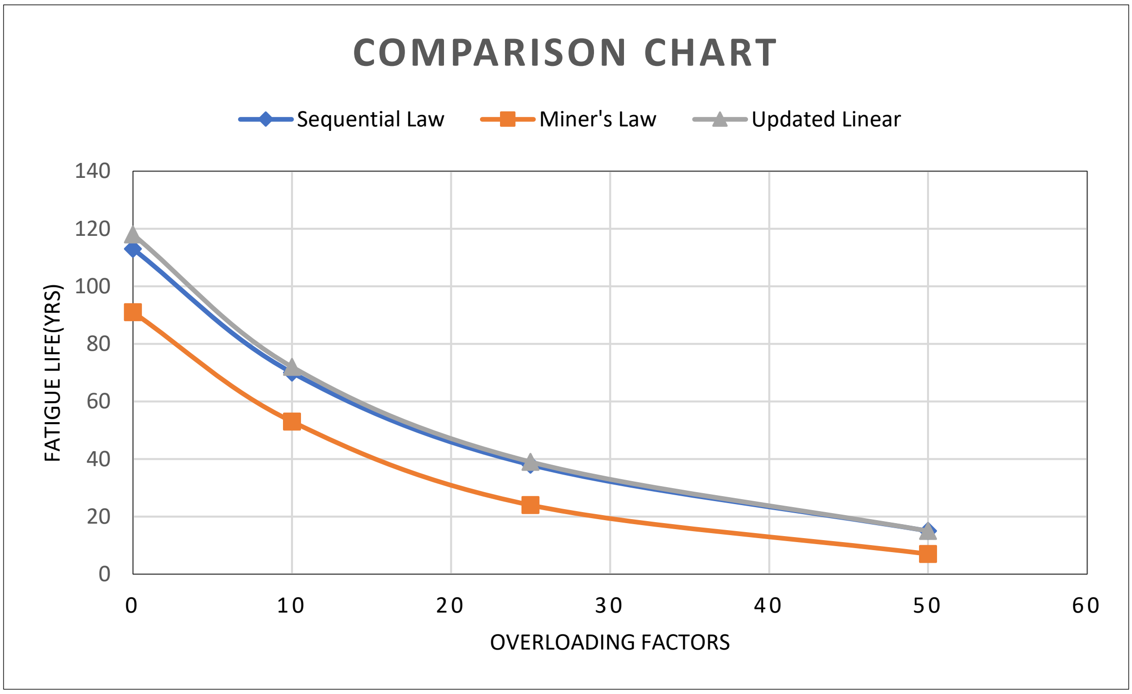

Figure 27: Life vs overloading factors

Table 16: Comparison of reduction in fatigue life

Fatigue Life (Years)						
Overloading factors	Sequential Law	% Reduction	Miner's Law	% Reduction	Updated Linear	% reduction
0	113	-	91	-	118	-
10	70	38.05	53	41.76	72	38.98
25	38	66.37	24	73.63	39	66.95
50	15	86.73	7	92.31	15	87.29
Nepal case	40.2	64.42	24	73.63	41.4	64.92

DISCUSSION OF RESULTS

The steepness in graph in damage of sequential law demonstrates that the damage is comparatively very high in later years than the early years. As fracture mechanics explains, for the first few years, the initiation of cracks in rebar does not occur. Once the crack initiates, the propagation of crack is rapid and the damage is exponential and the result shows the same. As stated earlier, the damage by Miner's rule is almost linear. Comparison results shows almost 22 years variation in fatigue life in no overloading condition for sequential law and Miner's law approach. Updated linear method where the damage is ratio of cycles acted to failure number of cycles from updated S-N curve is almost comparable to sequential law approach however, the fatigue progress is best represented by sequential law.

Different overloading conditions shows great variation in fatigue life. Table *16* shows the variation of fatigue life for different overloading conditions. Even 10% overloading condition can decrease fatigue life up to 38%, 25% overloading condition can decrease fatigue life up to 66% and 50% overloading can decrease fatigue life up to 86%. Considering the overloading condition existing in roads of Nepal, it was seen that the fatigue life decreased up to 64%. This shows that even low overloading can cause significant damage to the bridge. However, if there is no overloading condition, the fatigue life is greater than the design life of concrete, and thus problems due to fatigue may not occur.

CHAPTER SIX: CONCLUSION

6.1 Conclusions

In this thesis, the fatigue life of RCC T-Girder bridge is calculated by incorporating the sequential effect which appears due to loading of different amplitudes on bridges. For different vehicles, the stress time history is obtained at bridge deck. The concrete stress is converted to equivalent stress at reinforcement bars using limit state and sequential law is applied to carry out the fatigue damage. The fatigue damage due to Linear Damage Accumulation Rule (Miner's Rule) is also calculated and compared.

From the results obtained, it can be concluded that

1. The fatigue fracture life of reinforcement bars is 113 years by sequential approach and 91 years for linear damage approach.
2. The damage due to sequential law is comparatively low in initial years however there is exponential increase in damage in following few years.
3. The estimated fatigue life using sequential law is high as compared to Miner's damage so the result by linear rule is conservative.
4. Although the updated linear method seems to yield almost comparable result as sequential law, the fatigue progress is best represented by sequential law.
5. For 10%, 25% and 50% overloading conditions, the fatigue life were decreased by 38%, 66% and 86% respectively.
6. For overloading condition of road in Nepal, the overloading condition resulted in 64% decrease in fatigue life of bridge.

6.2 Further Recommendations:

1. It is recommended to consider stress concentration effect which would yield much realistic result of fatigue damage.
2. Experimental data retrieval through strain gauges in bridges would yield better results.

REFERENCES

Adasooriya , N. D., & Siriwardane , S. C. (2014). Remaining fatigue life estimation of corroded bridge members. *Fatigue and Fracture of Engineering Materials and Structures*, 603-622.

Aggarwal, V., & Parameswaran, L. (2015). Effect of Overweight Trucks on Fatigue Damage of a Bridge. *Springer*, 2483-2491.

Alampalli, S., & Lund, R. (2005). Estimating Fatigue Life of Bridge Components Using Measured Strains. *ASCE*, 725-736.

Arteaga, E. B., Bressolette, P., Chateauneuf , A., & Silva, M. S. (2008). Probabilistic lifetime assessment of RC structures under coupled corrosion–fatigue deterioration processes. *Elsevier*, 84-96.

Barnes, R., & Mays, G. (1999). “Fatigue performance of concrete beams strengthened with CFRP plates. *Journal of Composites for construction*, 63-72.

Bond, A., & Harris, A. (2008). *Decoding Eurocode 7.*

Charalambidi, B. G., Rousakis, T. C., & Karabinis, A. I. (2016). “Fatigue behavior of large-scale reinforced concrete beams strengthened in flexure with fiber-reinforced polymer laminates. *Journal of Composite for Construction*.

Dattoma, V., Giancane, S., Nobile, R., & Panella, F. W. (2005). Fatigue life prediction under variable loading based on a new non-linear continuum damage mechanics model. *Elsevier*, 89-95.

Deng, L., Yan, W., & Nie, L. (2018). A simple corrosion fatigue design method for bridges considering the coupled corrosion-overloading effects. *Elsevier*, 309-317.

Department of Transport Management. (2021). Axle load control: establishment of weighbridge stations along national highways. Department of Transport Management.

Elghazy, M., Refai, A. E., Ebead, U., & Nanni, A. (2018). Fatigue and Monotonic Behaviors of Corrosion-Damaged Reinforced Concrete Beams Strengthened with FRCM Composites. *ASCE*, 04018040-1 .

Heffernan, P. J., & Erki, M. A. (2001). Fatigue behaviour of reinforced concrete beams strengthened with carbon fiber reinforced plastic laminates. *Journal of Composites for Construction*, 132-140.

Kwon, K., Frangopol, D. M., & Soliman, M. (2012). Probabilistic Fatigue Life Estimation of Steel Bridges by using a Bilinear S-N Approach. *ASCE*, 58-70.

Leitao, F. N., Silva, J. S., & Andrade, S. A. (2012). Fatigue analysis and life prediction of composite highway bridge decks under traffic loading . *Latin American Journals of Solids and Structures*, 505-522.

Li, Z. X., Chan, T. H., & Ko, J. M. (2001). Fatigue damage model for bridge under traffic loading:application made to Tsing Ma Bridge. *Elsevier*, 81-91.

Ma, Y., Guo, Z., Wang, L., & Zhang, J. (2020). Probabilistic Life Prediction for Reinforced Concrete Structures Subjected to Seasonal Corrosion-Fatigue Damage. *ASCE*, 04020117-1-04020117-17.

Mesmacque, G., Garcia, S., Amrouche, A., & Gonzalez, C. R. (2004). Sequential law in multiaxial fatigue, a new damage indicator. *Elsevier*, 461-467.

Ni, Y. Q., Ye, X. W., & Ko, J. M. (2010). Monitoring-Based Fatigue Reliability Assessment of Steel Bridges: Analytical Model and Application. *ASCE*, 1563-1573.

Pokhrel, M. (2013). *Comparative Study of RCC T-Girder Bridge with Different Codes.* IOE, Pulchowk Campus.

Salem, A. (2013). *Dynamic Analysis and Fatigue Assessment of Bridge Decks Subjected to Traffic and Corrosion Effects.* Colorado: Colorado State University .

Schläfli, M., & Brühwiler, E. (1998). Fatigue of existing reinforced concrete bridge deck slabs. *Elsevier*, 991-998.

Siriwardane, S., Ohga, M., Dissanayake, R., & Taniwaki, K. (2007). Application of new damage indicator-based sequential law for remaining fatigue life estimation of railway bridges. *Elsevier*, 228-237.

SSEA. (1997). *Fatigue of concrete structures.* Zurich, Switzerland.

Stephens, R. I., Fatemi, A., Stephens, R. R., & Fuchs, H. O. (2000). *Metal fatigue in engineering* (2nd Edition ed.). New York: John Wiley and Sons.

V, S. M., R, A., & A, H. (2015). Fatigue Evaluation of Reinforced Concrete Highway Bridge. *International Journal of Innovative Research in Science,Engineering and Technology*, 2561-2569.

Wang, W., Deng, L., & Shao, X. (2016). Fatigue Design of Steel Bridges Considering the Effect of Dynamic Vehicle Loading and Overloaded Trucks. *ASCE*, 04016048-1-04016048-12.

Yang, D. H., Yi, T. H., & Li, H. N. (2017). Coupled Fatigue-Corrosion Failure Analysis and Performance Assessment of RC Bridge Deck Slabs. *ASCE*, 04017077-1 -04017077-9 .

Zhang, W., & Yuan, H. (2014). Corrosion fatigue effects on life estimation of deteriorated bridges under vehicle impacts. *Engineering Structure*, 128-136.

Zhongxiang, L., Tong, G., Hebdon, M. H., & Zhang, Z. (2018). Corrosion Fatigue Analysis and Reliability Assessment of Short Suspenders in Suspension and Arch Bridges. *ASCE*, 04018060-1 - 04018060-11 .

Zhou, Y. E. (2005). Assessment of Bridge Remaining Fatigue Life through Field Strain Measurement. *ASCE*, 737-744.

Traffic Controller. (n.d.). Retrieved July 3, 2020, from http://ssrn.aviyaan.com/traffic_controller/get_summary

APPENDIX

Sample Calculation

Fatigue Damage Calculation

σ_u= 485 Mpa

σ_1= 97.79Mpa

σ_2= 74.26 Mpa

σ_3= 67.41 Mpa

n_1 = 506255

n_2 = 910675

n_3 = 439825

N_1= 128656496

N_{1R}= 128150241

σ_{1ed}= 97.858

$D_1 = \frac{\sigma(1)ed - \sigma1}{\sigma u - \sigma1} = \frac{97.858 - 97.79}{485 - 97.79} = 0.000176$

$D'_2 = D_1 = 0.000176$

$\sigma'_{2ed} = D'_2(\sigma_u - \sigma_2) + \sigma_2 = 74.33$

N'_{2R}= 815708438

$N_{2R} = N'_{2R} - n_2 = 822071636$

σ_{2ed}= 74.34

$D_2 = \frac{\sigma(2)ed - \sigma2}{\sigma u - \sigma2} = \frac{74.34 - 74.26}{485 - 74.26} = 0.000198$

$\sigma'_{3ed} = D'_2(\sigma_u - \sigma_3) + \sigma_3 = 67.493$

N'_{3R}= 2675619482

$N_{3R} = N'_{3R} - n_3 = 2736906360$

σ_{3ed}= 67.49

$D_3 = \frac{\sigma(3)ed - \sigma3}{\sigma u - \sigma3} = \frac{67.49 - 67.41}{485 - 67.41} = 0.0002$

Stress on Rebar Calculation

Width of slab(b) = 1000mm

Location of neutral axis(x_0) = 41.04mm

Effective depth(h_o) = 179mm

Modular ratio(m) = 9

Area of cross section(A_o) = 565 mm^2

For LPK 2518 truck

σ_c= 2.784 Mpa

M^f_{max}= $1/2(\sigma^f_c*b*x_0*(h_o-x_o/3)$= 9444348.058 N-mm

$I^f(t) = b*x_o^3+ m*A_o*(h_o-x_o)^2$= 119906948.3 mm^4

$\Delta\sigma(t)$= $m*(M^f_{max}- M^f_{min})(h_o-x_o)/I^f(t)$= 97.796 Mpa

For LPK-1613 truck

σ_c= 2.114 Mpa

M^f_{max}= $1/2(\sigma^f_c*b*x_0*(h_o-x_o/3)$= 7171462.57 N-mm

$I^f(t) = b*x_o^3+ m*A_o*(h_o-x_o)^2$= 119906949.3 mm^4

$\Delta\sigma(t)$= $m*(M^f_{max}- M^f_{min})(h_o-x_o)/I^f(t)$= 74.26 Mpa

For LPO-1618 bus

σ_c= 1.919 Mpa

M^f_{max}= $1/2(\sigma^f_c*b*x_0*(h_o-x_o/3)$= 6509951.12 N-mm

$I^f(t) = b*x_o^3+ m*A_o*(h_o-x_o)^2$= 119906949.3 mm^4

$\Delta\sigma(t)$= $m*(M^f_{max}- M^f_{min})(h_o-x_o)/I^f(t)$= 67.41 Mpa